ROMANIAN ACADEMY

Institute of Physical Chemistry “Ilie Murgulescu”

**Alexandra-Teodora Toader (married Butnaru)**

PhD Thesis Abstract

# Oxide compounds of $nd^{10}$ elements with special electrical and optical properties

**Scientific adviser**

Academician PhD Maria Magdalena ZAHARESCU

Bucharest, 2016

# CONTENT of the PhD THESIS

# 1. INTRODUCTION

The oxide compounds of the metals are of particular interest due to their practical applications in various fields such as: electronics, optoelectronics, catalysis and refractory ceramics. Obtaining these materials at nanoscale dimensions, from the extended solid form to a particle of a material that contains a certain atoms resulted in outstanding variations of the optical, magnetic and electrical properties. Thus, the uses of these materials have expanded in: aerospace industry, cosmetics, electric motors, automotive industry, medicine and defense industry. This class of materials includes multilayer materials, nanocrystalline materials and nanocomposites materials. Their uniqueness is due to high percentage of the atoms at interfaces [1-2].

The term "nano" defines materials having at least one dimension of the order of $10^{-9}$ m, so that within this context in the category of nanomaterials [3] can be included any material consisting of very small particles containing a sufficient number of atoms of capable to modify the matrix properties.

Nanotechnologies represent the beginning of a revolutionary time in ability to control materials for the good of human society. Synthesis and control of the man-sized materials can lead to materials and devices with new features and properties. Nanotechnology [4] was defined as the ability to work at atomic, molecular and supramolecular scale, in the 1-100 nm range, in order to create, manipulate and use materials, devices and systems that have new properties and small functions due to their nanostructure.

Transparency in visible is an essential requirement for obtaining transparent conductive oxides a new class of materials with application in the production of solar cells, windows and electro chromic mirrors coatings, defrosting devices, furnaces, static dissipation, touch screens, electromagnetic shielding, invisible security circuits, etc.

The oxides of $3d^{10}$ (Cu, Zn, Ga) and $4d^{10}$(Ag, Cd, In şi Sn) elements, with d orbitals completly occupied have the values of band gap higher than 3,1 eV and they don’t exhibit transistions between energetic bands at energy lower than de 3,1eV. The abscence of the transitions at the values lower than 3,1eV confer to these oxides transparence in visible.

ZnO is one of the strongest candidates in a variety of electronic and semiconductor applications due to its low toxicity, low cost and its outstanding properties.

Preparation technologies both in liquid phase: sol-gel method [5], hydrothermal method [6] and in solid phase as mechanical-chemical activation have been reported for the synthesis of nanostructured oxide materials.

Taking in to account the arguments presented in the introduction regarding the properties of the oxides of $nd^{10}$ elements which exhibit properties of transparent conductive oxide the ***main objective*** of this thesis was the study of $ZnO\text{-}SnO_2$, $ZnO\text{-}Al_2O_3$ and Li, Ni doped ZnO systems.

Thus, ***the first research direction*** represented a complex study regarding phases formation and advanced ceramics obtained by solid state reactions for the compositions belonging to ***$ZnO\text{-}SnO_2$*** binary system. These studies were necessary taking into consideration the contradictory information in literatura data regarding the fomation of defined compounds and solid solubility limit of ZnO in $SnO_2$ and $SnO_2$ in ZnO.

***The second research direction*** was obtaining thin films in $ZnO\text{-}SnO_2$, $ZnO\text{-}Al_2O_3$, Sn, Li, Ni doped ZnO systems for potential applications as transparent conductive oxides. In the case of ***$ZnO\text{-}SnO_2$*** system thin films with the composition corresponding to $Zn_2SnO_4$ and $ZnSnO_3$ compounds that could be formed in $ZnO\text{-}SnO_2$ system and thin films corresponding to the individual oxides ($SnO_2$ şi ZnO) and doped ones were obtained.

**In the $ZnO\text{-}Al_2O_3$** system the preparation and characterization of Al doped ZnO thin films were studied. Different amounts of Al were used for films preparation in order to estabilish the optimum conditions for doping and obtaining improved optical and electrical properties.

In the Sn, Li and Ni doped ZnO system thin films with controlled type of conduction were obatined. The studied zinc oxide based TCO's films have been obtained by the sol–gel method and the prepared films were characterized from the structural and morphological point of view. Optical and electrical properties were also determined.

***The third research direction*** was to estabilishthe influence of the synthesis route on the formation mechanism of the ZnO nanopowders. ZnO powders were obatined in aqueos solution both by sol gel method and hydrotermal method. The obtained poweders were characterized in terms of thermal, structural and morphological properties.

The present thesis is structured in **3 Chapters** aiming to fulfil the proposed objectives.

**Chapter 1** provides general information regarding nanomaterials, especially about nanostructured metal oxides, emphasizing the requiered criteria for a material to be transparent conductor oxide. The oxides of $3d^{10}$ (Cu, Zn, Ga) and $4d^{10}$(Ag, Cd, In şi Sn)

elements meet these requirements which recomands them for possible applications as transparent conductive oxide, a direction less addressed.

Chapter 2 is divided in two subsections. In the first subchapter the main synthesis methods of the oxide materials are described, highlighting the methods which were the subject of this thesis**.** The second subchapter reports characterization methods of the oxide compounds in terms of thermal behaviour, structural, morphological and optical properties.

**Chapter 3** contains the most important results obtained in this thesis and it is divided in three subchapters corresponding to the three types of nanostructured oxide materials obtained: bulk (ceramic), thin films and powders.

## 2. ORIGINAL CONTRIBUTIONS

### 2.1. Oxide compounds formed in ZnO-$SnO_2$ binary system by solid state reaction [7, 8]

Ceramics belonging to ZnO-$SnO_2$ system are very intresting materials for applications such as: varistor, electrods, catalyst and gas sensor. Based on the serious discrepancies, that can still be found in the literature regarding the thermal evolution of the ZnO–$SnO_2$ binary system; in the present thesis a systematic study of the phase formation over the whole compositional range of the ZnO-$SnO_2$ binary system in the 500-1500 ºC temperature domain was approached. The phase formation was studied through solid state reaction method starting from comercial oxides. The powder mixtures of ZnO and $SnO_2$ were wet homogenized during 15 minutes in the agate mortar in absolute ethanol. Cylindrical samples were obtained by pressing at 100 MPa. The sample of (1-16) S/SZO (Table 1), were calcined at 500, 600, 800, 850, 900, 1000, 1100, 1150, 1200, 1300, 1400, 1500 $^{o}$C for 10 h. After thermal treatment all samples were cooled to room temperature with the furnace

In the experimental conditions beside initial oxides $SnO_2$ şi ZnO the presence of $Zn_2SnO_4$ (zinc stannate) was emphasized (Figs. 1, 2). The formation of $ZnSnO_3$ (zinc metastannate) mentioned in the literature data [9, 10] was not confirmed due to its limited thermal stability.

Zinc stannate was obtained even in non-izothermal conditions (heating rate of 10$^{o}$C/min) up to 1500 $^{o}$C, although the DTA analysis dosn't show any thermal effect. It seems that the interaction between two components take place in continouse mode at high temeparture.

Table 1 Composition and labelling of the studied samples

| Sample | Initial Composition (mol%) | | Sample | Initial Composition (mol%) | |
|---|---|---|---|---|---|
| | $SnO_2$ | ZnO | | $SnO_2$ | ZnO |
| $S_1$ (1SZO) | 100 | 0 | $S_9$(9SZO) | 40 | 60 |
| $S_2$(2SZO) | 97,5 | 2,5 | $S_{10}$(10SZO) | 33 | 67 |
| $S_3$(3SZO) | 95,0 | 5 | $S_{11}$(11SZO) | 30 | 70 |
| $S_4$(4SZO) | 90 | 10 | $S_{12}$(12SZO) | 20 | 80 |
| $S_5$(5SZO) | 80 | 20 | $S_{13}$(13SZO) | 10 | 90 |
| $S_6$(6SZO) | 70 | 30 | $S_{14}$(14SZO) | 5 | 95 |
| $S_7$(7SZO) | 60 | 40 | $S_{15}$(15SZO) | 2,5 | 97,5 |
| $S_8$(SZO) | 50 | 50 | $S_{16}$(16SZO) | 0 | 100 |

**Note**: Both denominations of the samples were used in the PhD Thesis

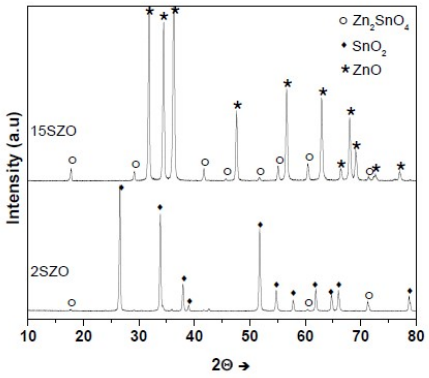


Fig. 1 XRD patterns of S2 and S15 samples thremally treated at1300 ºC.

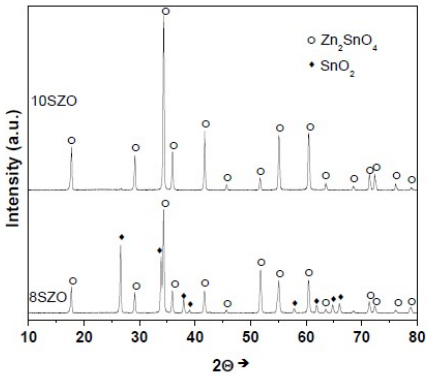


Fig. 2 XRD patterns of S8 and S10 samples thermally treated at 1300 ºC.

The microstructural parameters from XRD data for the selcetd samples were calculated (Table 2).

The results obtained by XRD measurements were confirmed by FT-IR spectroscopy. The FT-IR spectra of the starting oxides show typical absorption bands of $SnO_2$ [11] and ZnO lattice [12] (Figs.3, 4).

Table 2 Microstructural parameters from X-ray data for selected samples

| Sample | Phase composition | | Lattice parameters | | | c/a ratio | V (Å$^3$) | $D_c$(Å) | $R_{wp}$ | S |
|---|---|---|---|---|---|---|---|---|---|---|
| | Phase | (Wt %) | a(Å) | b(Å) | c(Å) | | | | | |
| $SnO_2^x$ | $SnO_2$ | - | 4,7382 | 4,7382 | 3,1871 | 0,6726 | 71,552 | | | |
| $ZnO^y$ | ZnO | - | 3,2539 | 3,2539 | 5,2098 | 1,6011 | 47,771 | | | |
| $Zn_2SnO_4^z$ | $Zn_2SnO_4$ | - | 8,6574 | 8,6574 | 8,6574 | 1 | 648,877 | | | |
| $S_1$ (1100$^0$C) | $SnO_2$ | 100 | 4,7377 | 4,7377 | 3,1877 | 0,6729 | 71,550 | 217 | 8,9 | 0,92 |
| $S_1$ (1300$^0$C) | $SnO_2$ | 100 | 4,7379 | 4,7379 | 3,1877 | 0,6728 | 71,577 | 232 | 9,7 | 1,01 |
| $S_2$ (1100$^0$C) | $SnO_2$ | 97,8 | 4,7376 | 4,7376 | 3,1864 | 0,6725 | 71,518 | 219 | 9,2 | 0,97 |
| | $Zn_2SnO_4$ | 2,2 | 8,6725 | 8,6725 | 8,6725 | 1 | 652,278 | 216 | | |
| $S_2$ (1300$^0$C) | $SnO_2$ | 97,7 | 4,7375 | 4,7375 | 3,1869 | 0,6726 | 71,526 | 225 | 11 | 1.11 |
| | $Zn_2SnO_4$ | 2,3 | 8,6664 | 8,6664 | 8,6664 | 1 | 650,899 | 213 | | |
| $S_8$ (1300$^0$C) | $SnO_2$ | 32,7 | 4,7340 | 4,7340 | 3,1870 | 0,6732 | 71,423 | 318 | 13,4 | 1,02 |
| | $Zn_2SnO_4$ | 67,3 | 8,6587 | 8,6587 | 8,6587 | 1 | 649,169 | 293 | | |
| $S_{10}$ (1300$^0$C) | $Zn_2SnO_4$ | 100 | 8,6581 | 8,6581 | 8,6581 | 1 | 649,034 | 233 | 10,2 | 1,14 |
| $S_{14}$ (1000$^0$C) | ZnO | 82,9 | 3,2492 | 3,2492 | 5,2140 | 1,6047 | 47,669 | 292 | 9,8 | 1,02 |
| | $Zn_2SnO_4$ | 17,1 | 8,6593 | 8,6593 | 8,6593 | 1 | 649,304 | 274 | | |
| $S_{15}$ (1100$^0$C) | ZnO | 90,3 | 3,2512 | 3,2512 | 5,2023 | 1,6001 | 47,621 | 231 | 7,4 | 1,05 |
| | $Zn_2SnO_4$ | 9,7 | 8,6581 | 8,6581 | 8,6581 | 1 | 649,032 | 205 | | |
| $S_{15}$ (1300$^0$C) | ZnO | 88,7 | 3,2508 | 3,2508 | 5,2040 | 1,6008 | 47,626 | 230 | 7,7 | 1,04 |
| | $Zn_2SnO_4$ | 11,3 | 8,6612 | 8,6612 | 8,6612 | 1 | 649,725 | 215 | | |
| $S_{16}$ (1100$^0$C) | ZnO | 100 | 3,2512 | 3,2512 | 5,2031 | 1,6003 | 47,628 | 240 | 7,4 | 1,05 |
| $S_{16}$ (1300$^0$C) | ZnO | 100 | 3,2511 | 3,2511 | 5,2044 | 1,6008 | 47,639 | 230 | 9,2 | 1,26 |

**Where**: (V) is the unit cell volume and (Dc) the mean crystallite size x data quoted from JCPDS file 00-041-1445; y data quoted from JCPDS file 01-080-0075; z data quoted from JCPDS file 00-024-1470; Rwp weighted difference between measured and calculated values, S show the goodness of the fit (1-1.5).

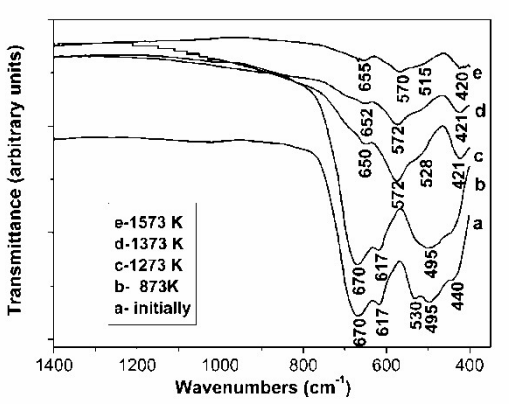


Fig. 3 FTIR spectra of S8 sample thermally treated at different temperatures

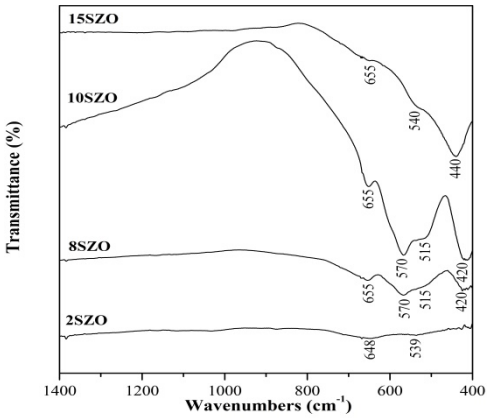


Fig. 4 FTIR spectra of the selected samples thermally treated at 1300 $^{o}$C/10h

Based on the obtained results presented it has been an attempt to draw the subsolidus phase relations in the $SnO_2$-ZnO (Fig. 5).

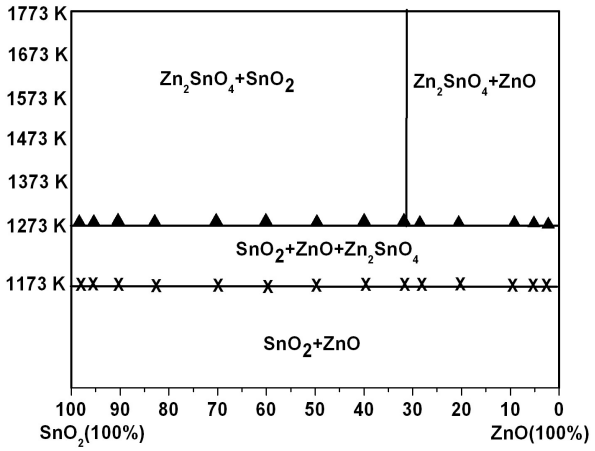


Fig.5 Subsolidus phase relations in the $SnO_2$-ZnO system

The formation of the $Zn_2SnO_4$ is noticed at 900 $^{o}$C. In the 900-1000 $^{o}$C temperature range a mixture of three phases is observed ($SnO_2$, ZnO, $Zn_2SnO_4$), while stating with 1000 $^{o}$C the presence of $Zn_2SO_4$ compound divides the binary system in two sub-systems, namely: $SnO_2$-$Zn_2SnO_4$ (0-66.6 mol% ZnO of the initial compositions) and $Zn_2SnO_4$-ZnO (66.6-100 mol% ZnO of the initial compositions). The increasing the temperature up to 1500 $^{o}$C did not changed the phase compositions.

The SEM images and grain size distribution of some selected sintered samples, namely $S_8$, $S_{10}$ and $S_{14}$ are presented in the Fig 6a-f. The selection was realized based on their composition and different sintering ability. The average grain sizes of the samples are: 2.06 (±0.4) for $S_8$, 4.26 (± 0.6) for $S_{10}$ and 2.9 (±0.8) μm for $S_{14}$. The SEM image of the $S_8$ sample confirms its low sintering ability showing the presence of a high porosity with all the pores connected. The $S_{10}$ sample is denser than the $S_8$ sample and shows both connected and also isolated (closed) pores located at the ceramic grain boundaries. The highest density was obtained for the sample $S_{14}$, which has only closed pores situated at the grain boundaries intersection, as it is shown in the SEM (Fig. 6e) and the TEM image (Fig. 7).

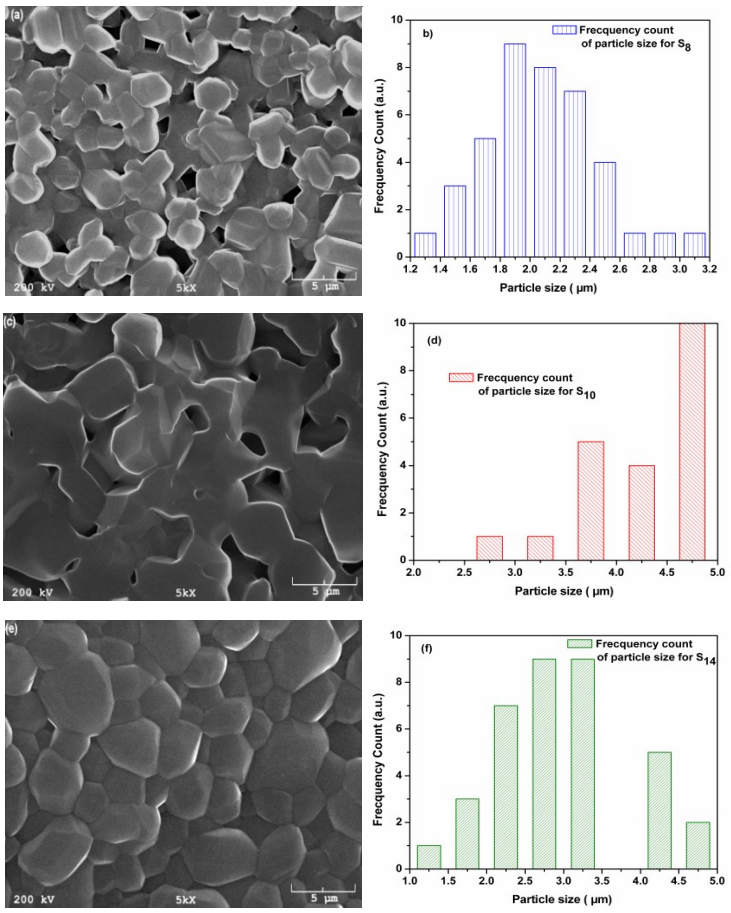


Fig 6 SEM images and grain size distribution: (a) SEM image of the $S_8$ sample; (b) grain size distribution of the $S_8$ sample; (c) SEM image of the $S_{10}$ sample; (d) grain size distribution of the $S_{10}$ sample; (e) SEM image of the $S_{14}$ sample; (f) grain size distribution of the $S_{14}$ sample.

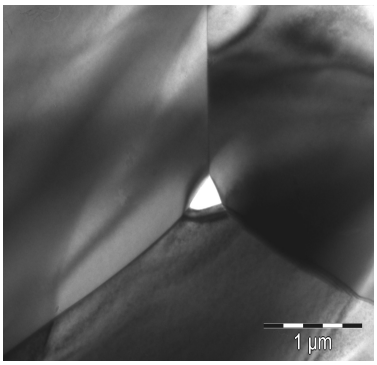


Fig. 7 TEM image of the $S_{14}$ sample

Impedance Spectroscopy technique was used to analyze the electrical characteristics which are important for a practical application of the selected samples (Fig. 8). In our experimental conditions, the impedance spectrum of the S10 sample shows only one semi-circle and the radius of the semi-circles become smaller with the increasing temperature, effect that is expected since current transport mechanisms are all thermally facilitated. Complex impedance spectrum of $S_{10}$ sample at 27 °C was fitted by using an equivalent circuit that includes three different contributions to the overall impedance: grain boundary, bulk, and electrode contact (Fig. 8b). All the investigated samples exhibit n-type semiconducting behaviour.

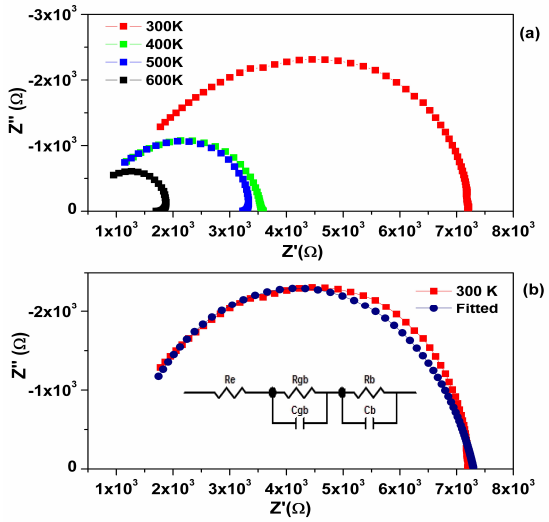


Fig. 8 Complex impedance spectra of $S_{10}$ sample at 27 °C, 127 °C, 227 °C şi 327 °C (a); Complex impedance spectrum of $S_{10}$ sample at 27 °C (b)

## 2.2. NAOSTRUCTURED FILMS BASED ON ZnO OBTAINED BY SOL- GEL METHOD

### 2.2.1. Films in the ZnO-$SnO_2$ system obtained by sol-gel method [13]

Films with Sn/Zn atomic ratio of 1:1 and 1:2 and and films with the following formula $Zn_{1-x}Sn_xO_{2-x}$ (where x=0; 0.025; 0.975; 1) were obtained by sol-gel method. The prepared solutions were stirred at 50°C for 120 minutes and stored at room temperature 24 hours before deposition by dip coating techniques on the glass and silicon substrates. The deposition conditions were: withdrawal speed 5 cm/min, withdrawal temperature 20 °C and the number of depositions 1-4 (for the films with Sn/Zn atomic ratio of 1:1 and 1:2) and 5-10 depositions (for $Zn_{1-x}Sn_xO_{2-x}$ films). Based on DTA/TG results of the gels resulted by gelfying of the prepared solustions, the obtained films were thermally treated at 500 °C for 5 min after each deposition. The final thermal treatment was realized at 500 °C for one hour. The obtained films showed a good adherence (without cracks) continuouse, homogeneous and exhibit a low roughness. The studied films were characterized from the morphological and structural point of view. The electrical and optical properties were, also determined.

X-Ray diffraction revealed the beginning of crystallization of both binary compounds zinc stannate ($Zn_2SnO_4$) and zinc metastannate ($ZnSnO_3$) (Figs. 9, 10).

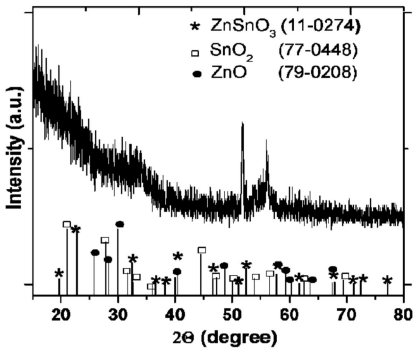


Fig. 9 XRD pattern of the film with atomic ratio Zn/Sn 1:1, deposited on silicon substrat

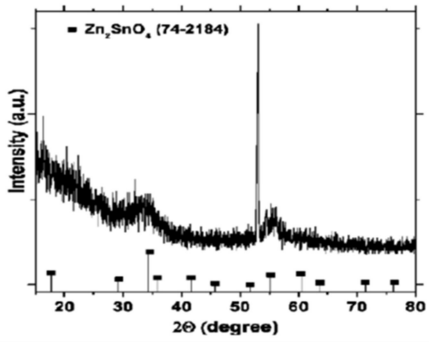


Fig.10 XRD pattern of the film with atomic ratio Zn/Sn 2:1, deposited on silicon substrat

The formation of $ZnSnO_3$ in the case of the films thermally treated at 500 ºC for 1 h is consistent with reported literatura data indicating that this compound can only be obtained by non conventional synthesis methods and its thermal stability is limited (below 600 $^oC$).

In the case of Sn doped ZnO and Zn doped $SnO_2$ the diffraction lines corresponding to the undoped oxide are observed (Figs. 11, 12).

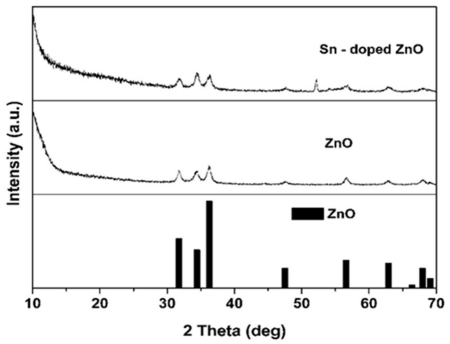


Fig.11 XRD patterns of the ZnO and Sn-doped ZnO films (10 layers)

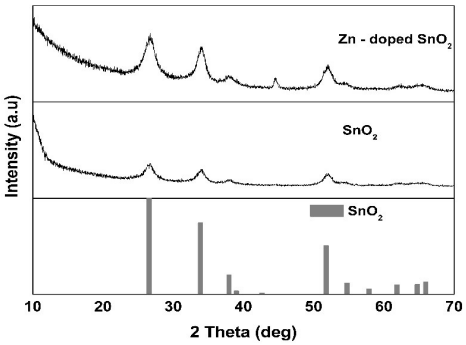


Fig.12 XRD patterns of the $SnO_2$ and Zn-doped $SnO_2$ films (10 layers)

Based on spectroelliposmtery measurements the refractive index (n) of the films deposited on the glass substrate 5 layers and 10 layers respectivley were obtained. The results are shown in Figs 13 and 14. It could be observed that the refractive indices increase by doping ZnO with Sn or $SnO_2$ with Zn.

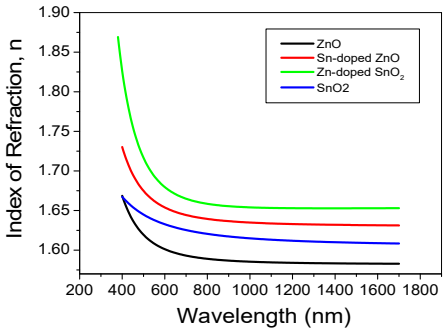


Fig. 13 Refractive index of TCO films 5 layers deposited on glass substrate

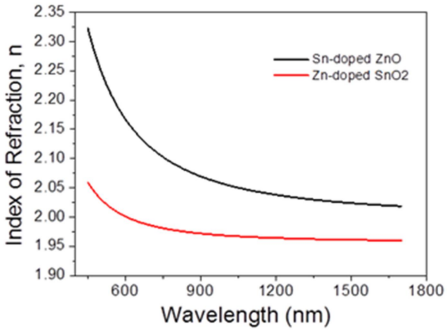


Fig. 14 Refractive index of TCO films 10 layeres deposited on glass substrate

The transmission coefficient of the films was found to be between 60-0% in agreement with the polycristalline structure of the films (wurtizte or rutile) and according to literature data [14].

### 2.2.2. Filme nanostructurate în sistemul $ZnO-Al_2O_3$ obţinute prin metoda sol-gel [15]

In the $ZnO-Al_2O_3$ system Al doped ZnO mono and multilayers films (with diffrent content of Al (0,5-5,0 % Al) were obatined by sol-gel method. The films were obtained using zinc acetate as source of zinc, aluminium nitrate and aluminium isopropoxide respectvley as aluminium source.

The obtained films after 5 layers deposition showed a good adherence (without cracks and exfoliations) and the roughness values obtained by AFM measurements are around 2 nm. All the films are polycrystalline with wurtzite type structure. The crystallite size calculated from XRD data is approx. 20 nm. The ZnO and Al doped ZnO films exhibit high electrical resistivity being not suitable for TCO applications but but could be of interest for acoustic resonators (FBAR).

### 2.2.3. ZnO based transparent conductive oxide films with controlled type of conduction [15]

Adherent and continuous doped (Sn, Li, Li\Ni) zinc oxide films as TCO materials deposited on glass and silicon substrates were obtained by the sol–gel method.

Optical, electrical structural and morphological properties of the studied films depend on chemical composition of the solutions, number of depositions and the type of substrate.

The structural characterization of the synthesized films was realized by X-ray diffraction measurements. The XRD pattern of the undoped ZnO based film obtained by 10 layers deposition is presented in Fig. 15. XRD indicates that all the obtained films are polycrystalline with the hexagonal ZnO wurtzite-type structure. The change of lattice parameters could be attributed to the small atoms incorporation (Sn, Li, Ni) into the ZnO lattice by substituting on the original lattice sites (e.g. Zn). This result was confirmed by XRF and XPS measurements.

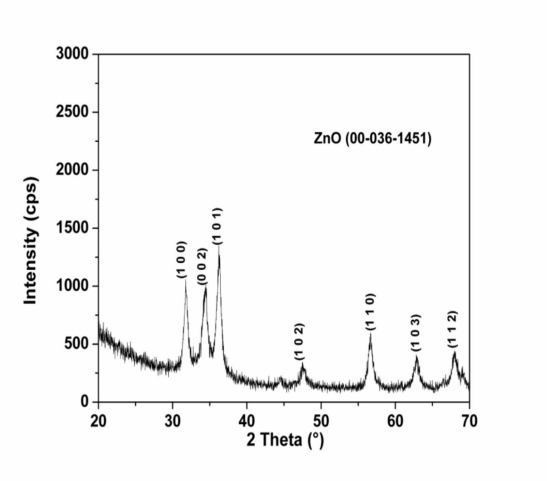


Fig. 15 XRD pattern of $ZO_{S\text{-}10}$ film

The morphology of Li doped ZnO ($LZO_{S\text{-}5}$) in the micro-scale (Fig. 16, left part, up) is similar with that of the undoped ZnO film ($ZO_{S\text{-}5}$), with particle sizes and interparticle superficial porosity in the nano-scale. Particle and pore sizes are about 10 nm in the outer surface (Fig. 16, left part, down), and significantly coarser, about 30 nm, inside the film, shown in the internal cross-section images in Fig. 16, right.

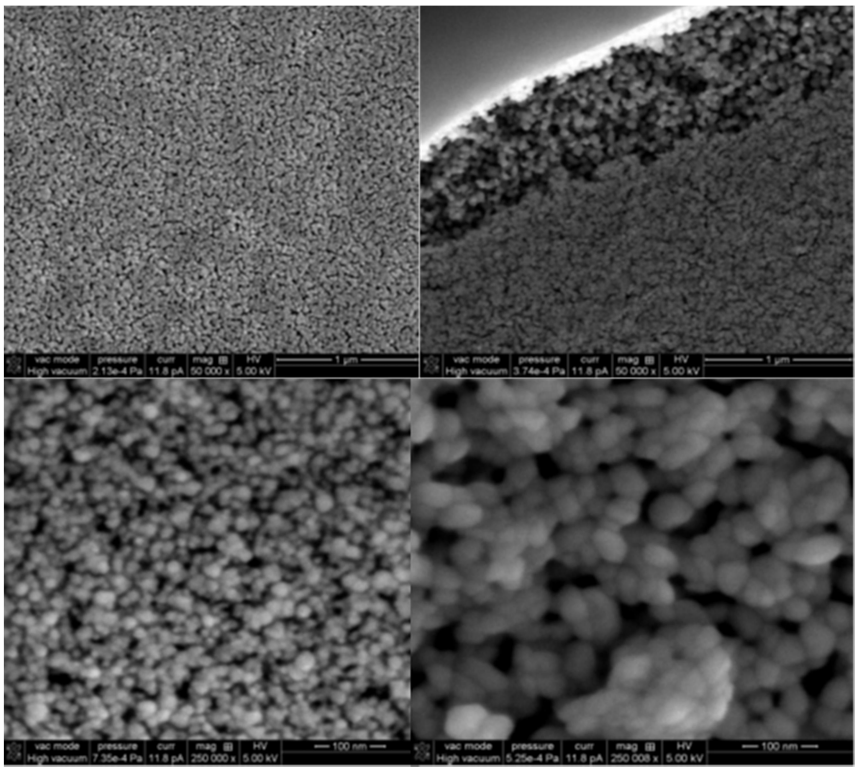

Fig.16 SEM micrographs showing the typicalmicrostructure of undoped ZnO films: (top left) surface morphology showing the micro-scale porosity; (top right) cross section, showing the internal microstructure of the nanoparticulate porous films; (bottom left) detail of the outer surface morphology showing the particle size and interparticle porosity; and (bottom right) detail of the microstructure inside the film.

The EDX elemental analysis detected only Zn and O in the film, corresponding to ZnO composition, the light element Li being out of the range of EDX detection, as illustrated by the spectra in Fig. 17.

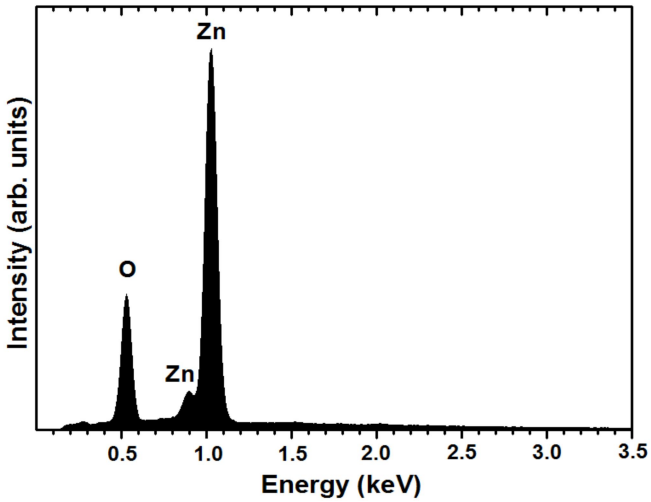


Fig. 17 EDX spectrum of the ZnO film.

***Electrical characterization.*** The doped and un-doped ZnO thin films were electrically investigated by Hall measurements in order to determine the conduction type, resistivity (ρ), carrier concentration ($N_D$) and mobility (μ) and Seebeck measurements to establish conductivity type and Seebeck coefficients (α).The results are presented in Table 3.

**Tabel 3** Electrical properties of the studied samples

| *Sample* | Conduction type | $N_D$ ($cm^{-3}$) | ρ (□cm) | μ ($cm^2$/Vs) | □ (□V/K) |
|---|---|---|---|---|---|
| $ZO_{G-5}$ | n | $5.48x10^{14}$ | 4340 | 2.6 | - |
| $TZO_{G-10}$ | n | $1.48x10^{17}$ | 129 | 0.33 | - |
| $LZO_{G-5}$ | n | $1.04x10^{15}$ | 3550 | 1.7 | - |
| $LZO_{S-5}$ | p | $1.83x10^{16}$ | 234 | 145 | +188 |
| $LNZO_{G-5}$ | n/p | $3.28x10^{14}$ | 2100 | 9.1 | +135 |
| $LNZO_{S-5}$ | p | $6.75x10^{16}$ | 2.41 | 38.6 | +186 |
| $LNZO_{G-10}$ | p | $8.69x10^{14}$ | 1840 | 3.9 | +169 |

The comparative evaluation of the electrical properties of all studied films led to the conclusion that un-doped ZnO as well as Sn-doped ZnO exhibit **n**-type conduction. Li-doped ZnO films present **n**-type or **p**-type semiconducting behavior according to the type of substrate. The codoping of the ZnO with two cations (Li and Ni) leads to the formation of the films with **p**-type conduction, no matter the type of substrate (glass or Si/SiOx) used.

## 3.ZnO NANOSTRUCTURED POWDERS OBTAINED FROM AQUEOUS SOLUTIONS [6]

In order to obtain ZnO nanostructured materials, gels and precipitates starting from aqueos solutions of $Zn(NO_3)_2{\cdot}nH_2O$ (ZAH) and $(CH_2)_6N_4$ (HMTA) with a molar ratio of 4:1 and 2:1 respectivley were synthetized.

In the case of hydrothermal treatment of $Zn(NO_3)_2{\cdot}nH_2O$(ZAH)-$(CH_2)_6N_4$ (HMTA) solution with molare ratio of 2:1 heated at 90 $^oC$ for 12 hours ZnO nanorods with higher cristalinity degree than that of the powder were obtained.

The obtained samples were characterized by XRD, FTIR spectroscopy and scanning electron microscopy.

The XRD pattern reveals that the as-synthesized product is the pure hexagonal wurtzite phase of ZnO in agrrement with the JCPDS card No.00-36-1451 (Fig. 18).

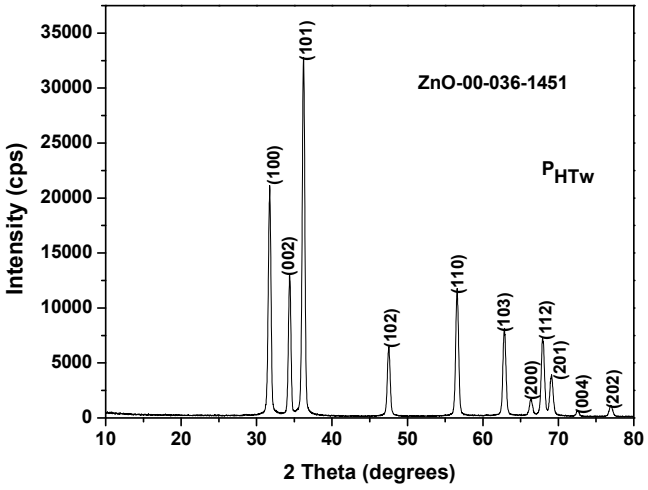


Fig. 18 XRD pattern of $P_{HTw}$ sample

In our experimental conditions (with small content of HMTA), through the hydrothermal method, ZnO powder of well faceted hexagonal micro rods elongated along **c**-axis have been obtained (Fig.19).

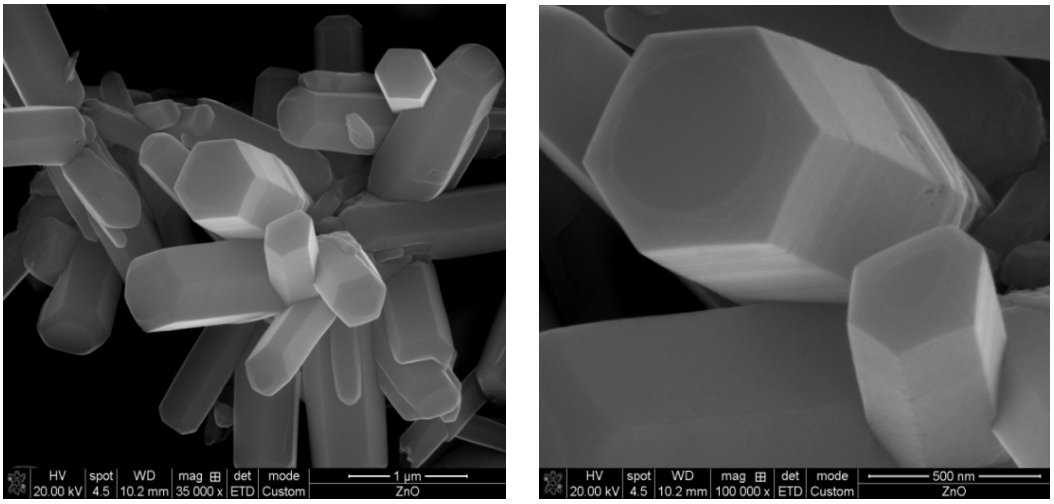


Fig.19 SEM images of the $P_{HTw}$ sample.

## 4.CONCLUSIONS

The PhD thesis aimed to obtain oxide combinations of $nd^{10}$ elements with improved optical and electrical properties. Among the $nd^{10}$ elements the study of ZnO and $SnO_2$ as individual oxides or in policomponent oxide systems such as: ZnO-$SnO_2$, ZnO-$Al_2O_3$, Li doped ZnO and Li, Ni co-doped ZnO was approached.

**In the ZnO-$SnO_2$ binary system,** a systematic study on the phase formation over the whole compositional range in the 500-1500 $^oC$ temperature domain was reported. The investigated samples were prepared by solid state reaction.

The structure, morphology and electrical properties of the thermally treated $SnO_2$-ZnO samples were investigated by XRD and FT-IR measurement leading to the conclusion that in the studied system, only $Zn_2SnO_4$ binary compound is formed.

Starting with 900 ºC temperature the formation of the $Zn_2SnO_4$ with inverse spinel type structure was emphasized in all samples. The formation of the $ZnSnO_3$ was not observed in the experimental conditions used.

Based on the structural results the sub-solidus equilibrium phase diagram was established. The presence of the $Zn_2SnO_4$ compound divides the system in two subsolidus domains: $SnO_2$-$Zn_2SnO_4$ and $Zn_2SnO_4$-ZnO.

All studied samples belonging to ZnO-$SnO_2$ system exhibit n type semiconductor behaviour as resulted from impedance measurements.

In the same oxide system films obtained by sol-gel method and deposited by dip coating onto glass and Si/SiOx substrates with the similarly compositions to that of binary compounds **(**$Zn_2SnO_4$ and $ZnSnO_3$) or of the doped oxides (ZnO, Sn doped ZnO, $SnO_2$, Zn doped $SnO_2$).

In the case of the films thermally treated at 500 $^oC$ for 1 h XRD patterns revealed the formation of both binary compounds zinc stannate ($Zn_2SnO_4$) and zinc metastannate ($ZnSnO_3$). Thus, the literature data regarding the formations of $ZnSnO_3$ were confirmed indicating that this compound can only be obtained by non conventional synthesis methods and its thermal stability is limited (below 600 $^oC$).

**In the ZnO-$Al_2O_3$** system Al doped ZnO mono and multilayers films (with diffrent content of Al (0,5-5,0 % Al) were obatined by sol-gel method. The films were obtained using zinc acetate as source of zinc, aluminium nitrate and aluminium isopropoxide respectvley as aluminium source.

The ZnO and Al doped ZnO films exhibit high electrical resistivity being not suitable for TCO applications but could be of interest for acoustic resonators (FBAR).

**The Li doped ZnO and Li, Ni co-doped ZnO films** showed good transmittance (70–90%) from visible to near-IR range. By co-doping ZnO with Li\Ni, p-type semiconducting behaviour was found (by Hall and Seebeck measurements) on both glass and Si wafer substrates, which was maintained even after 4 months storage.

În cazul obtinerii de materiale **nanostructurate de ZnO în soluţii apoase**, s-au sintetizat gelurile şi precipitatele din soluţii apoase în sistemul $Zn(NO_3)_2{\cdot}nH_2O$ (ZAH) - $(CH_2)_6N_4$ (HMTA), cu rapoarte molar de 4:1 sau 2:1.

In the case of ZnO nanostructured materials, gels and precipitates starting from aqueos solutions of $Zn(NO_3)_2{\cdot}nH_2O$ (ZAH) and $(CH_2)_6N_4$ (HMTA) with a molar ratio of 4:1 and 2:1 respectivley were synthetized.

In the case of hydrothermal treatment of $Zn(NO_3)_2{\cdot}nH_2O$(ZAH)-$(CH_2)_6N_4$ (HMTA) solution with molare ratio of 2:1 heated at 90 $^oC$ for 12 hours ZnO nanorods with higher cristalinity degree than that of the powder were obtained.

**References (selection):**

[1]. H. Gao, G. Fang, M. Wang, N. Liu, L. Yuan, C. Li, L. Ai, J. Zhang, C. Zhou, S. Wu, X. Zhao, *Mater. Res. Bull.*, *43*, 3345-3351, **2008**

[2]. P. Uthirakumar , J.H.Kang, S.Senthilarasu, C.-H.Hong *Physica E*, **,** *43,* 1746-1750, **2011**

[3]. L.-Y.Yang, S.-Y.Dong, J.-H. Sun, J.-L. Feng, Q.-H. Wu, S.-P.Sun, *J. Hazardous* Mat.**,** *179,* 438-443, 2**010**

[4]. M.C. Roco, *J. Nanopart. Res.,* **1**, 435, **1999**.

[5]. M. Zaharescu, S. Mihaiu, **A. Toader**, I. Atkinson, J. Calderon-Moreno, M. Anastasescu, M. Nicolescu, M. Duta, M. Gartner, K. Vojisavljevic, B.Malic, V.A. Ivanov, E.P. Zaretskaya, *Thin Solid Films* 571, 727–734, **2014.**

[6]. S. Mihaiu, O. C. Mocioiu, **A. Toader**, I. Atkinson, J. Pandele Cuşu, C. Munteanu,M. Zaharescu*„ Rev. Roum. Chim.*, **2013**.

[7]. S. Mihaiu, I. Atkinson, O. Mocioiu, **A. Toader**, E. Tenea, M. Zaharescu, *Rev.Roum.Chim*. **56**, 465-469, **2011.**

[8]. S. Mihaiu, **A. Toader**, I. Atkinson, O. C. Mocioiu, C. Hornoiu., V. S. Teodorescu, M. Zaharescu, *Ceram. Int*., 41, 4936-4945, **2015.**

[9]. Y.S. Shen and T. Zhang, *Sens. Actuators B Chem.*, *12* , 5, **1993.**

[10]. D. Kovacheva and K. Petrov, *Solid State Ionics, 109*, 327, **1998.**

[11]. J. Fayat and M.S. Castro, *J. Eur.Ceram.Soc*., *23,*1585, **2003.**

[12]. W. Cun, X.M. Wang, J. C. Zhao, B. X. Mai, G.Y. Sheng, P. A .Peng, J .M. Fu, *J. Mater. Sci.*, **37,** 2989-2996, **2002.**

[13]. **A. Toader**, S. Mihaiu, M. Voicescu, M. Anastasescu, H. Stroescu, M. Nicolescu, I. Atkinson, M. Gartner, M. Zaharescu, Advanced Topics in Optoelectronics, Microelectronics, and Nanotechnologies VI, edited by Paul Schiopu, Razvan Tamas, Proc. of SPIE Vol. 8411, **2012**

[14]. S. Mihaiu, I. Atkinson, M. Anastasescu, **A. Toader**, M. Voicescu, M. Zaharescu, R*ev.Roum.Chim*., 57(4-5), 477-490, **2012.**

[15]. M.S. Mihaiu, **A. Toader**, M. Anastasescu, M. Gabor, T. Petrisor jr., M. Stoica, M. Zaharescu, Proc.Appl.Ceram., 3, 79-84, **2009.**